arXiv:hep-ph/0109010v2 24 Oct 2001

Saturation and geometric scaling in DIS at small x

Krzysztof Golec-Biernat‡

II Institute of Theoretical Physics, Hamburg University, Germany
Institute of Nuclear Physics, Kraków, Poland

Abstract. We present various aspects of the saturation model which provides good description of inclusive and diffractive DIS at small x. The model uses parton saturation ideas to take into account unitarity requirements. A new scaling predicted by the model in the small x domain is successfully confronted with the data.

1. Introduction

Deeply inelastic electron-proton scattering (DIS) at small value of the Bjorken variable x ($\ll 1$) attracted a lot of attention, mostly due to the experimental results from HERA. From the theory side, the small-x DIS opens a new kinematic regime for the QCD studies. The predicted by QCD, and confirmed by the data [1], strong rise of the proton structure functions with decreasing x is the indication that at small x the proton structure is dominated by dense gluon systems. In DIS at moderate values of x, the linear QCD evolution equations lead to good description of this process, explaining scaling violation. At small x, however, the problem is more complicated since recombination processes between partons in a dense system have to be taken into account. At the formal level, these processes allow to restore unitarity of the DIS cross sections as $x \to 0$, violated in the QCD description based on the linear evolution equations, by taming the rise of the parton distributions. This effect is called *parton saturation* [2].

It was unclear for a long time whether recombination processes (or unitarization procedures in general) are important in the HERA kinematic range. Most of the analyses of this problem were based on the results obtained in the double logarithmic approximation in which x is small but Q^2 is large. The linear evolution equations in this case are modified by non-linear terms describing parton recombination. In such approximation it was found that the impact of non-linearity is either small or masked by the choice of initial conditions for the linear evolution [3].

The breakthrough came from realization that the proper starting point is the high energy QCD factorization formula for the structure functions, derived under the assumption that x is small but Q^2 is arbitrary (provided $Q^2 \gg \Lambda^2$ and pQCD is justified). This allows to find the necessity for unitarity, realized in the spirit of parton saturation, in the transition from DIS to small Q^2 scattering [4]. The full potential of

‡ golec@mail.desy.de

the unitary description is revealed for diffractive DIS [5]. In particular, the constant ratio of diffractive to total DIS cross sections as a function of x and Q^2 is naturally explained.

The approach we are going to present is partially phenomenological. We take into account several important features of parton saturation in the parameterization of the QCD interactions in a dense gluon system, especially the existence of a saturation scale. The proposed parameterization is very efficient in the description of the data and may serve as a guidance for the detailed QCD studies.

2. Saturation model

The saturation model was formulated and compared at length to DIS data in [4, 5]. Here we describe this model, discussing some details which were not presented in the original formulation. For related approaches see [6].

In the rest frame of the proton, the QCD description of DIS at small x can be interpreted as a two-step process. The virtual photon (emitted by the incident electron) splits into a $q\bar{q}$ dipole which subsequently interacts with the proton. The proton structure function F_2 results from the high energy QCD factorization theorem. In terms of virtual photon-proton cross sections $\sigma_{T,L}$ for the transverse and longitudinal polarized photons [7]

$$F_2(x,Q^2) \,=\, Q^2/4\pi^2\alpha_{em}\,(\sigma_T \,+\, \sigma_L) \tag{1}$$

and

$$\sigma_{T,L} \,=\, \int d^2\mathbf{r}\,dz\,|\Psi_{T,L}(\mathbf{r},z,Q^2)|^2\;\hat{\sigma}(x,r), \tag{2}$$

where $\Psi_{T,L}$ is the light-cone *wave function* of the virtual photon and $\hat{\sigma}$ is the *dipole cross section* describing the interaction of the $q\bar{q}$ dipole with the proton. In equation (2) $\mathbf{r}$ is the transverse separation of the $q\bar{q}$ pair and z is the photon's momentum fraction carried by the quark, see Figure 1. Thus $(\mathbf{r},z)$ are good quantum numbers conserved by the interaction in the considered approximation.

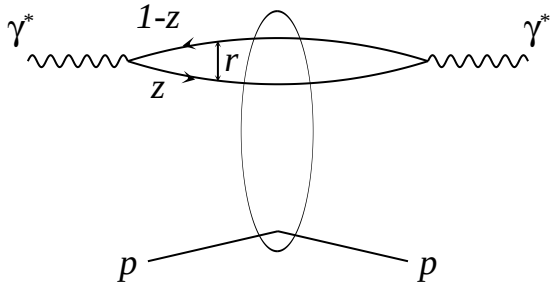


Figure 1. *Schematic representation of the basic factorization in inclusive DIS at small x.*

The photon wave functions are known from pQCD, e.g. for transverse photons and massless quarks

$$|\Psi_T(\mathbf{r}, z, Q^2)|^2 \;=\; \frac{3\,\alpha_{em}}{2\pi^2}\,\sum_f e_f^2\,[z^2+(1-z)^2]\;\overline{Q}^2\,K_1^2(\overline{Q}r), \tag{3}$$

where $\overline{Q}^2 \;=\; z(1-z)\,Q^2$ and K_1 is the Bessel function. The computation of the dipole cross section $\hat{\sigma}$ has been attempted within pQCD assuming different types of net colourless gluon exchange (e.g. DGLAP or BFKL ladders). Most of these attempts, however, are plagued by problems with unitarity of finally computed cross sections.

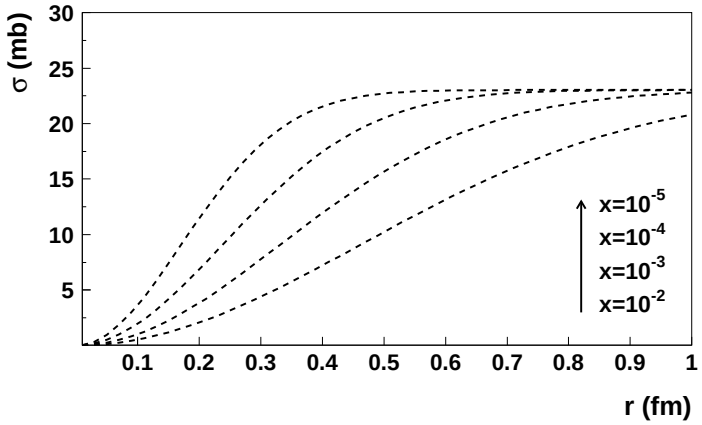


Figure 2. Dipole cross section for different values of x.

In our approach we built in unitarity in the dipole cross section by proposing the following phenomenological form

$$\hat{\sigma}(x,r) = \sigma_0\,\left\{1-\exp\left(-\frac{r^2}{4R_0^2(x)}\right)\right\}, \tag{4}$$

with $R_0(x)$, called saturation radius, given by

$$R_0^2(x) = \frac{1}{Q_0^2}\,\left(\frac{x}{x_0}\right)^{\lambda}, \tag{5}$$

where $Q_0^2 = 1$ GeV^2. The parameters $\sigma_0 = 23$ mb, $x_0 = 3\cdot 10^{-4}$ and $\lambda = 0.29$ were found from the fit to all inclusive DIS data at $x < 0.01$. At small r, $\hat{\sigma}$ features colour transparency, $\hat{\sigma} \sim r^2$, which is purely pQCD phenomenon. For large r, saturation occurs, $\hat{\sigma} \simeq \sigma_0$. The fact that $\hat{\sigma}$ is limited by the energy independent cross section may be regarded as a unitarity bound. The transition between the two regimes is governed by $R_0(x)$. As illustrated in Figure 2, for $x \to 0$ the transition occurs for decreasing transverse sizes. This is an essential feature of parton saturation pioneered by the analysis [2] in which internal saturation scale $Q_s(x)$ appears. We built in such a scale into our model: $Q_s(x) \sim 1/R_0(x)$.

With the proposed dipole cross section we achieved good description of the DIS data at small x, including the transition to small Q^2 values, see Figure 3. The reason for this can be easily understood after performing the following qualitative analysis.

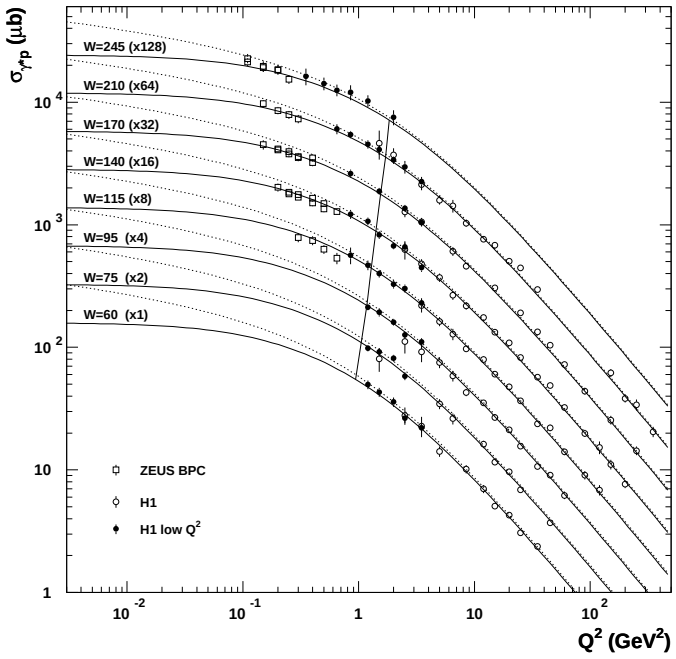


Figure 3. $\sigma_{\gamma^* p} = \sigma_T + \sigma_L$ for different energies W of the $\gamma^* p$ system. The solid lines show the fit results with a light quark mass $m_f = 140$ MeV while the dotted lines with $m_f = 0$. The line across the curves indicates the position of the critical line.

3. Qualitative analysis

We concentrate on the transverse cross section σ_T which dominates in F_2. The dominant contribution to σ_T results from the behaviour of the Bessel function in (2): $K_1(x) = 1/x$ for $x \ll 1$ while for $x \gg 1$, $K_1(x)$ is exponentially suppressed. Thus using (3),

$$\sigma_T \;\sim\; \int_0^\infty \frac{dr^2}{r^2} \int_0^1 dz\, \left[z^2 + (1-z)^2\right]\, \hat{\sigma}(x,r)\, \Theta\big[z(1-z)\, Q^2 r^2 < 1\big]\,, \qquad (6)$$

where $\Theta(x < 1)$ equals 1 if $x < 1$, or 0 otherwise. For $0 \le r \le 2/Q$, the theta function does not impose any restriction on z and the z-integration gives a constant. Such a configuration, called *symmetric*, is rather uniform in z with the mean value 1/2. For large transverse separations, $r \gg 2/Q$, the theta function heavily restricts z to small values: $z < 1/(Q^2 r^2)$. Now, the z-integration gives the factor $2/(Q^2 r^2)$. In this configuration, called *aligned jet*, z or $(1-z) \approx 0$. Thus, one of the quarks follows the photon direction while the other stays with the proton.

Finally, we obtain

$$\sigma_T \;\sim\; \underbrace{\int_0^{4/Q^2} \frac{dr^2}{r^2}\, \hat{\sigma}(x,r)}_{symmetric} \;+\; \underbrace{\int_{4/Q^2}^\infty \frac{dr^2}{r^2}\, \left(\frac{1}{Q^2 r^2}\right)\, \hat{\sigma}(x,r)}_{aligned\ jet}, \qquad (7)$$

where we neglected multiplicative numerical factors. For the forthcoming analysis let us approximate (6) by

$$\hat{\sigma}(x,r) \;=\; \begin{cases} \sigma_0\, r^2/4R_0^2(x) & \text{for} \quad r \le 2R_0(x) \\ \\ \sigma_0 & \text{for} \quad r > 2R_0(x)\,, \end{cases} \tag{8}$$

which form contains all essential features of the exact formula. The leading Q^2-behaviour of σ_T depends on the relation between two scales: the *characteristic size* of the $q\bar{q}$ dipole $1/Q$ and the *mean transverse distance* between partons given by $R_0(x)$.

If the partonic system is dilute $1/Q \ll R_0(x)$, and from (7,8) we find

$$\sigma_T \;\sim\; \underbrace{\frac{\sigma_0}{Q^2R_0^2}}_{r<2/Q} \;+\; \underbrace{\frac{\sigma_0}{Q^2R_0^2}\,\ln\left(Q^2R_0^2\right)}_{2/Q<r<2R_0} \;+\; \underbrace{\frac{\sigma_0}{Q^2R_0^2}}_{r>2R_0}\,, \tag{9}$$

where we indicated the r-integration regions. In terms of the structure function (1) we obtain scaling with logarithmic violation. Notice that all dipole sizes, including those from the non-perturbative region, contribute to scaling. The assumption that $R_0^2 \sim x^\lambda$ leads to the power-like behaviour, $F_2 \sim x^{-\lambda}$, observed in the data.

When the system of partons becomes dense for the dipole probe and $1/Q \gg R_0(x)$, a different behaviour is found

$$\sigma_T \;\sim\; \underbrace{\sigma_0}_{r<2R_0} \;+\; \underbrace{\sigma_0\,\ln\left(\frac{1}{Q^2R_0^2}\right)}_{2R_0<r<2/Q} \;+\; \underbrace{\sigma_0}_{r>2/Q}\,. \tag{10}$$

Now, the structure function is in agreement with unitarity: $F_2 \sim Q^2\,\sigma_0\,\ln(1/x)$. The change of the behaviour of σ_T from (9) to (10) when Q^2 increases while W^2 stays fixed ($x = Q^2/W^2 \to 0$) is shown in Figure 3. The same transition is obtained in the Regge limit of DIS, Q^2 fixed and $W^2 \to \infty$, since the $\gamma^* p$ center-of-mass energy W enters the description only through the Bjorken variable x.

The transition between the scaling and unitary behaviour of the structure function depends on x and occurs in the region of the (x, Q^2)-plane marked by the *critical line*: $1/Q = R_0(x)$. In our interpretation, at the critical line the characteristic size of the dipole probe equals the mean transverse separation between partons. The characteristic feature of parton saturation is that the transition occurs at increasing values of Q^2 when $x \to 0$. We found that at HERA the transition region is situated for $Q^2 \approx 1 - 2$ GeV^2, which justifies the use of pQCD.

4. Photoproduction limit

It is interesting to consider a formal limit $Q^2 \to 0$ in the saturation model. The analyzed cross sections are divergent in this limit if $m_f = 0$. However, if a non-zero quark mass is assumed, the limit can be performed and we find for $m_f^2 \gg Q^2 \to 0$,

$$\sigma_T \;\sim\; \sigma_0\,\ln\left(\frac{1}{m_f^2R_0^2(x)}\right)\,, \tag{11}$$

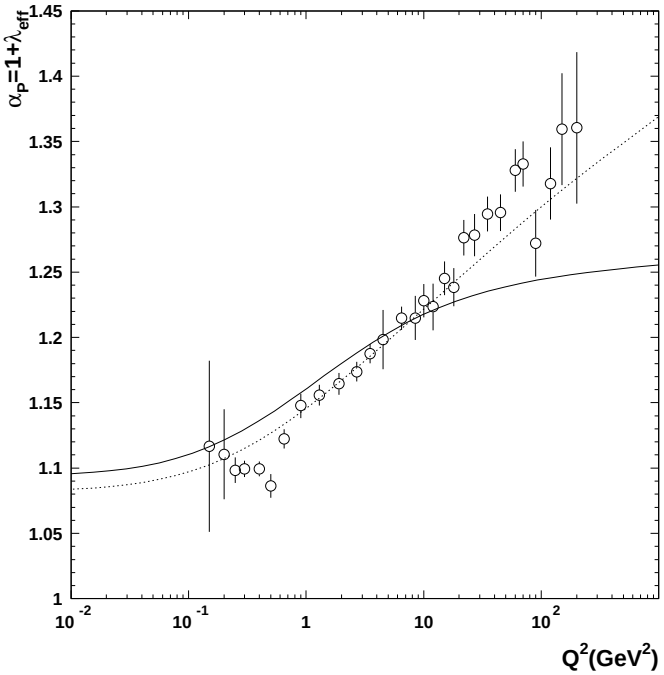


Figure 4. The effective pomeron intercept $\alpha_P = 1 + \lambda$ as a function of Q^2, found from the dependence: $\sigma_{\gamma * p} \sim (W^2)^{\lambda}$. The solid line corresponds to the saturation model (4) while the dashed line shows the effect when the model is modified to include the DGLAP evolution (Section 6). The data points are from ZEUS.

$$\sigma_L \;\sim\; \sigma_0 \, \frac{Q^2}{m_f^2} \,, \tag{12}$$

where we additionally modify the Bjorken variable formula to allow for the photoproduction limit

$$x \;=\; \frac{Q^2 + 4m_f^2}{W^2} \,. \tag{13}$$

As expected, the longitudinal cross section vanishes when $Q^2 = 0$. We also see that m_f plays a crucial role for the value of the transverse cross sections. In our analysis we set $m_f = 140$ MeV to obtain good agreement with the HERA photoproduction data. For $Q^2 \gg m_f^2$, the light quark mass does not play a significant role.

From the discussion in Section 3 we know that the energy dependence of σ_T changes from $\sigma_T \sim (W^2)^{\lambda}$ for large Q^2 to $\sigma_T \sim \ln(W^2)$ in the photoproduction limit. It appears that for each Q^2 we can effectively parameterize the energy dependence through the power-like behaviour: $\sigma_T \sim (W^2)^{\alpha_P(Q^2)-1}$. The found dependence $\alpha_P(Q^2)$ is shown in Figure 4. Interestingly, $\alpha_P(Q^2)$ interpolates between the soft and hard pomeron intercept values.

5. Geometric scaling

Let us realize that the dipole cross section (4) is a function of the combination $r/R_0(x)$ instead of x and r separately,

$$\hat{\sigma}(x,r) \,=\, \hat{\sigma}(r/R_0(x)). \tag{14}$$

This has profound consequences for the total cross section $\sigma_{\gamma^* p} = \sigma_T + \sigma_L$, if the quark mass m_f in the photon wave functions is neglected. Rescaling the integration variable $r \to r/R_0$ in (2), we find that $\sigma_{\gamma^* p}$ becomes a function of the dimensionless variable $\tau = Q^2\, R_0^2(x)$, being the ratio of the two geometric scales discussed in Section 3,

$$\sigma_{\gamma^* p}(x,Q^2) \,=\, \sigma_{\gamma^* p}\big(Q^2 R_0^2(x)\big)\ . \tag{15}$$

The non-zero light quark mass, introduced to extrapolate the model down to the photoproduction region, does not lead to a significant breaking of a new scaling (which we call geometric scaling) in the small x domain [8]. So does the charm contribution, discussed in detail in [4]. In Figure 5, reproduced from [8], we illustrate geometric scaling for the small-x data in a broad range of Q^2.

In its essence, geometric scaling is a manifestation of the presence of the internal saturation scale characterizing a dense partonic system, $Q_s(x) \sim 1/R_0(x)$. The presence of such scale emerges from a pioneering work of [2], which was subsequently analyzed and generalized in [9]. In reference [10] the scaling property similar to that postulated in the dipole cross section (4) was found and analyzed in detail in [11].

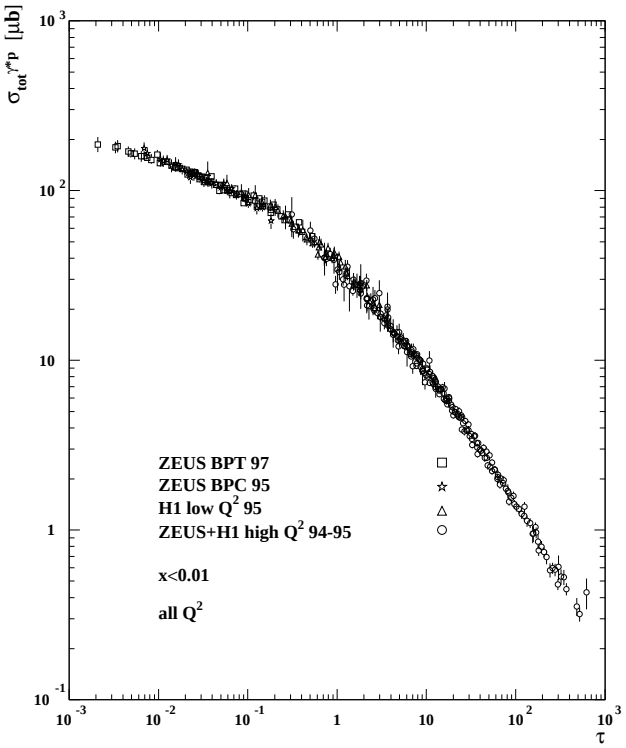


Figure 5. *Experimental data on $\sigma_{\gamma^* p}$ from the region $x < 0.01$ plotted versus the scaling variable $\tau = Q^2 R_0^2(x)$. Q^2 values are between* 0.045 *and* 450 GeV^2.

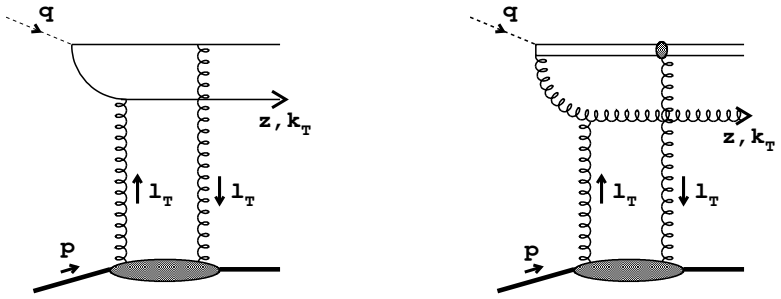


Figure 6. Diffractive $q\bar{q}$ and $q\bar{q}g$ contributions.

6. DGLAP evolution in the saturation model

In the limit of large Q^2 values, the structure function (1) is dominated by the small size transverse contribution. In this limit, the high energy formula (1) should make a contact with the DGLAP formula for F_2. This allows to find the following relation between the dipole cross section at small r and the ordinary gluon distribution [12],

$$\hat{\sigma}(x,r) \approx \frac{\pi^2}{3}\, r^2\, \alpha_s\, xg(x, C/r^2). \tag{16}$$

The gluon distribution $g(x,\mu^2)$ obeys the DGLAP evolution equations. The parameter C in (16), as well as the argument of α_s, cannot be determined in the considered leading $\log Q^2$ approximation.

In the saturation model (4), $\hat{\sigma} \sim r^2/R_0^2(x)$ at small r. Thus the logarithmic dependence on r, resulting from the DGLAP evolution of the gluon, is not included in the model. In our recent analysis [13] we include the DGLAP evolution by proposing the following modification of the saturation model

$$\hat{\sigma}(x,r) = \sigma_0 \left\{ 1 - \exp\left(-\frac{\pi^2\, r^2\, \alpha_s(\mu^2)\, xg(x,\mu^2)}{3\,\sigma_0} \right) \right\}, \tag{17}$$

where the scale $\mu^2 = C/r^2 + \mu_0^2$, and the parameters C and μ_0^2 are determined from the best fit to the DIS data. Additionally, two parameters of the initial gluon distribution: $xg = A_g\, x^{-\lambda_g}$ are fitted. The result of the comparison with the data is shown in Figure 4 as the dotted line. As expected, the proper DGLAP limit of $\hat{\sigma}$ significantly improves agreement at large values of Q^2 without affecting the physics of saturation responsible for the transition to small Q^2. The full discussion of the results will be presented in [13].

7. Saturation and DIS diffraction

DIS diffraction, $\gamma^* p \to pX$, is a good test of the parton saturation ideas incorporated in (4). In the simplest case the diffractive system X, well separated in rapidity from the scattered proton, consists of the $q\bar{q}$ pair. This contribution dominates for the diffractive mass $M^2 \sim Q^2$. In the large diffractive mass limit, $M^2 \gg Q^2$, additional components like $q\bar{q}g$ have to be taken into account. These two components are shown in Figure 6.

The cross section for the diffractive $q\bar{q}$ production reads [7]

$$\frac{d\,\sigma^D_{T,L}}{dt}_{|\,t=0} \;=\; \frac{1}{16\,\pi}\int d^2\mathbf{r}\,dz\,|\Psi_{T,L}(\mathbf{r},z)|^2\;\hat{\sigma}^2(x,\mathbf{r}), \tag{18}$$

where t is the squared momentum transfer to the diffractive system. Assuming exponential dependence on t, $e^{B_D t}$, we divide (18) by the diffractive slope B_D (taken from the experiment) to obtain the total cross section $\sigma^D_{T,L}$. The dipole cross section $\hat{\sigma}$ is given by the saturation model (4) which parameters were determined by the inclusive structure function analysis. Thus, the description of diffractive DIS (for $M^2 \sim Q^2$) is parameter free and differs from the inclusive one by the squared dipole cross section.

We can perform a qualitative analysis using the formulae from Section 3. In the DIS case, when $1/Q \ll R_0(x)$, we find for the diffractive $q\bar{q}$ production from transverse photons

$$\sigma^D_T \;\sim\; \underbrace{\frac{\sigma_0^2}{Q^4R_0^4}}_{r<2/Q} \;+\; \underbrace{\frac{\sigma_0^2}{Q^2R_0^2}}_{2/Q<r<2R_0} \;+\; \underbrace{\frac{\sigma_0^2}{Q^2R_0^2}}_{r>2R_0}. \tag{19}$$

By the comparison with (9), we see that the leading scaling result comes from large transverse sizes. The contribution from $r < 2/Q$ is suppressed by the additional power of Q^2 (higher twist contribution). Notice that the DGLAP modification of the dipole cross section for small r does not influence the leading result. Therefore, DIS diffraction is strongly sensitive to the region of the transition to saturation in the dipole cross section (4). In fact, the saturated form of $\hat{\sigma}$ is necessary for the observed in the data constant ratio σ^D/σ^{tot}. Considering the leading contribution to (9) and (19), we find

$$\frac{\sigma^D}{\sigma^{tot}} \;\sim\; \frac{1}{\ln(Q^2R_0^2(x))}, \tag{20}$$

which is a slowly varying function of x and Q^2.

Summarizing the qualitative analysis, by exposing the semi-hard ($2/Q < r < 2R_0$) and non-perturbative ($r > 2R_0$) regions, DIS diffraction is an ideal process to test parton saturation realized in terms of the dipole cross section (4). The constant ratio σ^D/σ^{tot} as a function of x and Q^2 finds a natural explanation in the saturation model.

In [5] we perform an extensive comparison of the saturation model predictions with the data by modelling the diffractive state as shown in Figure 6. Good agreement is found for both the H1 and ZEUS data. In particular, in Figure 7 we show the energy ($x_{I\!P}$) dependence of the diffractive structure function which is determined by the energy dependence found in the inclusive structure function analysis. In particular, away of the region $M^2 \ll Q^2$ ($\beta \to 1$) where the higher twist longitudinal $q\bar{q}$ component dominates, we find for the leading twist part of the diffractive structure function

$$F_2^D \;\sim\; x_{I\!P}^{1-2\alpha_P}, \tag{21}$$

where the "effective pomeron intercept" $\alpha_P = 1+\lambda/2 \approx 1.15$ (λ is defined in Section 2). This value is in remarkable agreement with the experimental values: 1.17 by H1 [14] and 1.13 by ZEUS [15].

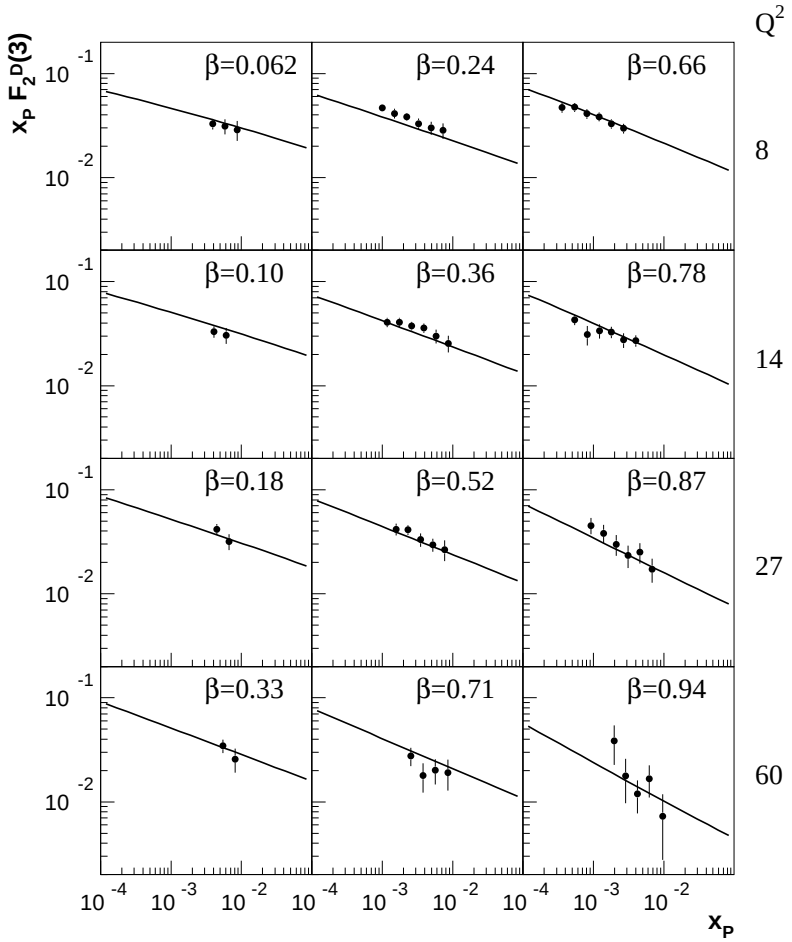


Figure 7. *The diffractive structure functions $F_2^{D(3)}(\beta, Q^2, x_{I\!P})$ as a function of $x_{I\!P} = (Q^2 + M^2)/(Q^2 + W^2)$ for different values of $\beta = Q^2/(Q^2 + M^2)$ and Q^2 (in units of GeV^2). The data are from ZEUS [15].*

We have to add, however, that the treatment of the $q\bar{q}g$ component, interacting with the proton with the same dipole cross section (up to a colour factor) as the $q\bar{q}$ system, goes beyond the saturation model since this component is not present in the inclusive analysis. More detailed studies are necessary.

The presented model of DIS diffraction can be extended to include more complicated diffractive states, e.g. with partons strongly ordered in transverse momenta (DGLAP configuration). In this case initial diffractive parton distributions are directly computed from the saturation model and subsequently evolved using the DGLAP evolution equations. The results are presented in [16].

8. Conclusions

The idea of parton saturation realized through the proposed model of the dipole cross section turns out to be very successful in the unified description of inclusive and diffractive DIS at small x. In particular, the transition to small Q^2 in inclusive DIS,

the constant ratio σ^D/σ^{tot} and the energy dependence of diffractive DIS are naturally obtained in the presented approach. From a formal point of view, these ideas allow to obey unitarity of the description. The detailed QCD picture of the discussed processes is still a matter of intensive theoretical studies. From a phenomenological point of view the most promising is the analysis done in [10, 17] in which multiple pomeron exchanges are responsible for saturation as postulated in our model. In this case the dipole cross section (or better the $q\bar{q} - p$ forward scattering amplitude) obeys a non-linear evolution equation. Therefore, the future offers an exciting time for new developments.

Acknowledgments

I am grateful to the organizers of the Ringberg Workshop for their kind invitation and for an excellent organization. I warmly thank J. Bartels, H. Kowalski, M. W. Krasny, J. Kwieciński, K. Peters, S. Riess, A. Staśto and particularly M. Wüsthoff for enjoyable collaboration on the subject of this presentation. I also thank E. Łobodzinska for careful reading of the manuscript. This research has been supported in part by the EU Fourth Framework Programme "Training and Mobility of Researchers" Network, "Quantum Chromodynamics and the Deep Structure of Elementary Particles", contract FMRX-CT98-0194 (DG 12-MIHT) and by the Polish KBN grant No. 5 P03B 144 20. The Deutsche Forschungsgemeinschaft fellowship is gratefully acknowledged.

References

[1] H1 Collaboration, Adloff C et al., 2001 *Eur. Phys. J.* C **21** 33
ZEUS Collaboration, Chekanov S. et al. 2001 *Eur. Phys. J.* C **21** 443
[2] Gribov L V, Levin E M and Ryskin M G 1983 *Phys. Rep.* **100** 1
[3] Bartels J, Schuler G. A and Blümlein J 1991 *Z. Phys.* C **50** 9
Golec–Biernat K, Krasny W and Riess S 1994 *Phys. Lett.* B **337** 367
[4] Golec–Biernat K and Wüsthoff M 1999 *Phys. Rev.* D **59** 014017
[5] Golec–Biernat K and Wüsthoff M 1999 *Phys. Rev.* D **60** 114023
[6] Forshaw J R, Kerley G and Shaw G 1999 *Phys. Rev* D **60** 074012, 2000 *Nucl. Phys.* A **675** 80
Gotsman E, Levin E M, Maor U and Naftali E 1999 *Eur. Phys. J.* C **10** 689
Cvetic G, Schildknecht D and Shoshi A 1999 *Acta Phys. Polon.* B **30** 3265
McDermott M, Frankfurt L, Guzey G and Strikman M 2000 *Eur. Phys. J.* C **16** 64
[7] Nikolaev N N and Zakharov B G 1990 *Z. Phys.* C **49** 607, 1992 *Z. Phys.* C **53** 331
Mueller A H 1994 *Nucl. Phys.* B **415** 373, 1995 *Nucl. Phys.* B **437** 107
[8] Staśto A M, Golec-Biernat K and Kwieciński J 2001 *Phys. Rev. Lett.* **86** 596
[9] Mueller A H and Qiu J 1986 *Nucl. Phys.* B **268** 427
Mueller A H 1990 *Nucl. Phys.* B **335** 115
Levin E M and Bartels J 1992 *Nucl. Phys.* B **387** 617
McLerran L and Venugopalan R 1994 *Phys. Rev.* D **49** 2233, 1994 *Phys. Rev.* D **49** 3352
Venugopalan R 1999 *Acta Phys. Polon.* B **B30** 3731
Iancu E, Leonidov A and McLerran L 2001 *Nucl. Phys.* A **692** 583
Iancu E and McLerran L 2001 *Phys. Lett.* B **510** 145
Jalilian-Marian J, Kovner A, McLerran L and Weigert H 1997 *Nucl. Phys.* B **504** 415, 1999 *Phys. Rev.* D **59** 014014, 1999 *Phys. Rev.* D **59** 034007

Balitsky I. I 1996 *Nucl. Phys.* B **463** 99, 1999 *Phys. Rev.* D **60** 014020, `hep-ph/0101042`, 2001 *Phys. Lett.* B **518** 235
Weigert H `hep-ph/0004044`
Ferreiro E, Iancu E, Leonidov A, McLerran L `hep-ph/0109115`
Mueller A. H `hep-ph/0110169`
[10] Kovchegov Yu V 1999 *Phys. Rev.* D **60** 034008, 2000 *Phys. Rev.* D **61** 074018
[11] Levin E M and Tuchin K 2000 *Nucl. Phys.* B **573** 833, 2001 *Nucl. Phys.* A **691** 779, 2001 *Nucl. Phys.* A **693** 787
Levin E M and Lublinsky M `hep-ph/0104108`, `hep-ph/0108239`
Lublinsky M 2001 *Eur. Phys. J.* C **21** 513
[12] Frankfurt L, Miller G A and Strikman M 1993 *Phys. Lett.* B **304** 1
Frankfurt L, Radyushkin A and Strikman M 1997 *Phys. Rev.* D **55** 98
[13] Bartels J, Golec-Biernat K and Kowalski H *in preparation*
[14] H1 Collaboration, Adloff C et al. 1997 *Z. Phys.* C **76** 613
[15] ZEUS Collaboration, Derrick M et al. 1999 *Eur. Phys. J.* C **6** 43
[16] Golec–Biernat K and Wüsthoff M 2001 *Eur. Phys. J.* C **20** 313
[17] Kovchegov Yu V and Levin E. M 2000 *Nucl. Phys.* B **577** 221